Brazilian Journal of Physics (2023) 53:16
https://doi.org/10.1007/s13538-022-01229-x

GENERAL AND APPLIED PHYSICS

Pc5 Pulsations in the South Atlantic Magnetic Anomaly

Edwin Camacho[1,2] · Luiz Benyosef[1] · Odim Mendes[2] · Margarete Oliveira Domingues[2]

Received: 24 August 2022 / Accepted: 17 November 2022 / Published online: 5 December 2022

Abstract
This paper investigates the Pc5 magnetic pulsation characteristics influenced by the South Atlantic Magnetic Anomaly (SAMA) in a moderate geomagnetic storm through records analysis of geomagnetically conjugate stations interlinking both hemispheres. This study uses the horizontal magnetic components measured in the same time interval in two typical longitudes: the America-SAMA region and Asia-Pacific one, whose stations are under equivalent McIlwain L-parameter (L-shell). Our procedure uses those data recorded simultaneously in six conjugate-station pairs to identify and characterize the Pc5 pulsation. The methodology integrates spectral analyses based on fast Fourier transform and wavelet transform techniques, obtaining signal characterizations and coherence analysis to highlight the Pc5 pulsation dynamics. As a result, work found that Pc5 pulsations showed simultaneous and similar patterns in the occurrence intervals in the Asia-Pacific region, reinforcing previous results from more restricted research. Concerning the America-SAMA region, the Pc5 pulsation amplitudes in the Northern hemisphere stations presented pulsation amplitudes following the Asia-Pacific amplitude behavior. The pulsation amplitudes were higher in the SAMA region than those in the Northern hemisphere. Also, in the SAMA, concerning the conjugate stations, Pc5 pulsation presents the highest energy values in the typical Pc5 spectra during storm intervals with higher intensity. Between the conjugate pairs, pulsations showed moderate to low signal coherences and phase lags.

Keywords South Atlantic Magnetic Anomaly · Pc5 pulsations · Wavelet transform · Coherence analysis · Space weather

1 Introduction

The South Atlantic Magnetic Anomaly (SAMA) is nowadays one of the most critical features of the Earth's magnetic field. This anomaly extends from the East Pacific to South Africa, covering latitudes between 15° and 45° [1, 2], in which the main magnetic field has a significant low intensity of the order of 22,000 nT, approximately one-third compared to the maximum magnetic field value [1, 3, 4]. Sanchez et al. [5] located the SAMA minimum value currently in northern Argentina, considered its center, which has historically displaced from Southern Africa to South America over the last 300 years [4, 6].

The mechanisms involved in the generation of the SAMA have not yet been identified. Generally, two models are proposed as the possible generation mechanisms. In the first model, the origin is commonly attributed to the eccentric dipole offset towards the northwest Pacific [7, 8]. In the second model, which stresses a main internal contribution, the cause is a patch of opposite magnetic flux compared to the dipole direction at the core-mantle boundary (CMB) [2, 4, 9]. A CMB inverse flux patch has been growing continuously from the beginning of the nineteenth century, in a behavior highlighted by a decrease of the dipolar field and a significant increase of the non-dipolar field in the Southern Atlantic [2, 10]. Some authors even propose the current SAMA expansion interpretation as an indicator of an impending reversal of terrestrial magnetic field [11–13]. A consequence of the significant magnetic magnitude reduction in this

Luiz Benyosef, Odim Mendes and Margarete Oliveira Domingues are authors contributed equally to this work.

✉ Edwin Camacho
edwincmch@gmail.com

Luiz Benyosef
benyosef@on.br

Odim Mendes
odim.mendes@inpe.br

Margarete Oliveira Domingues
margarete.domingues@inpe.br

[1] COGE, National Observatory - ON, R. Gen. J. Cristino, 77, Rio de Janeiro 20921-400, RJ, Brazil

[2] National Institute for Space Research - INPE, Av. Astronautas, 1758, São José dos Campos 12227-010, São Paulo, Brazil

region is that high-energy Van-Allen-radiation-belt particles penetrate deeper into the upper atmosphere in this region than anywhere else on the Earth [14]. This high-radiation zone has a potential threat to low Earth-orbiting satellites, such as weather-forecast satellites, and human-crewed missions when passing through the SAMA [7, 9, 15, 16]. Due to the electrodynamics acting upon this region, some effects have also been detected on the surface as disturbances in communications and induced currents in pipelines, transmission lines, and power grids [6, 17]. Currently, it is known the development of a second minimum within the SAMA at Earth's surface and it has been observed in the southwest of Africa, at around 5°W, 40°S, firstly reported by Terra-Nova et al. [18]. Green's functions relating the core-mantle boundary radial field to the surface intensity show this feature is connected with the movement and evolution of a reversed flux feature under South Africa [19].

Also, other significant phenomena that occur within the region dominated by the geomagnetic field are Pc5 magnetic pulsations, characterized as ultra-low-frequency (ULF) magnetohydrodynamic (MHD) waves, with frequencies between 1.6 and 7 mHz, often observed during intervals of disturbances on the geomagnetic field. Studies on magnetic pulsations are essential to extend a knowledge of their characteristics and effects inside the magnetosphere-ionosphere system [20–22]. Essentially, waves can resonate with the dynamics (gyrating, bouncing, and drifting behaviors) of the particles, which could be scattered or even lost to the atmosphere. Similarly, waves can obtain energy from the particles affecting the characteristics of the waves, even producing plasma instabilities [23, 24]. Therefore, the steps of identifying, characterizing, and understanding the pulsations are indispensable efforts to support investigations on how they are generated and even a way to obtain information about the regions through which they propagate and in which processes they participate. Although many studies have been done about magnetic pulsations, there are gaps of information to be considered and analyzed, such as better characterizations of pulsations and their dynamics concerning occurrences mainly at middle and low latitudes [25, 26]. To sum up, the magnetic pulsations analysis helps us understand the energy transfers between areas of different latitudes through waveguides and magnetic flux lines, even eventual interactions with charged particles, both in the ionosphere and in the upper regions [20].

In this work, we focus on magnetic pulsations Pc5 for their ability to assist in the diagnosis of the electrodynamic environment of the magnetosphere-ionosphere system [27, 28]. They have been studied using magnetic data both from ground stations [29–31] and satellites [22, 32]. Their generation is commonly associated with external and internal sources [33]. The most frequently cited external source of Pc5 pulsations in the magnetosphere is the Kelvin-Helmholtz instability at its external boundary, designated as magnetopause [34, 35]. Pc5 pulsations have also been related to the magnetosphere compression by the solar wind pressure associated with the increasing of a magnetopause current and the occurrences of Storm Sudden Commencements (SSC) and Sudden Impulses (SI) [36–38]. Besides those causes, two internal sources have also been proposed for generating pulsations: the magnetic Field Line Resonance, known as FLR, and the cavity/waveguide modes [30, 33, 39–42].

Contributing to those studies, including to consider the influence of the ionosphere itself, a significant possibility is to evaluate the simultaneous pulsations at geomagnetically conjugated points at low latitudes. For this work, a signal analysis approach, supported on the suggestions given by [30] and [43], enables to mitigate the external influence of the solar wind and magnetosphere interaction. Besides studying the own Pc5 pulsations characterization, a study strategy based on geomagnetically conjugate stations can help in investigating somehow the role of the ionosphere and plasmasphere in Pc5 processes [39, 44].

Two points on the Earth's surface, each located at a distinct geomagnetic hemisphere, are considered geomagnetically conjugate if they are on opposite ends of the same geomagnetic field line [45, 46]. In principle, geophysical phenomena generally exhibit a similar behavior during an event or a phenomenon in a delimited area around the conjugate points [45]. Nagata et al. [47] and Wescott [48] showed that there is a very close correlation of magnetic activity in the time of occurrence, form, and amplitude in magnetic signals (H component) in conjugate points. Pulsations were also studied in conjugate points and, specifically, Pc5 showed similar and symmetrical behavior, oscillating in phase and with similar amplitudes [36, 39, 45, 46, 49]. Most of the studies related to conjugate stations are investigations using data collected at high and middle latitudes [30, 39, 44, 46–48, 50–52]. Few results, most of them facing limitations in analysis techniques, have been reported from conjugate station data at low latitudes. Some research examples are Wescott and Mather [50] and Yumoto et al. [53], where they studied the H component variations and examined the characteristics of Pc3 magnetic pulsations, respectively.

Motivated by those studies, a fundamental question could be investigated here to extend the knowledge in the area: *How different are the Pc5 pulsation characteristics recorded in conjugate stations affected by the SAMA?* The main objective of this paper is to analyze data from conjugate stations both at middle-to-low latitudes, with L-shell $\leq$ 2, and at the SAMA region, during a geomagnetic storm. For our case study, the magnetic data used were simultaneously recorded at six conjugate pair stations. Three pair stations are located in the America-SAMA region, and the other pairs are located in the Asia-Pacific region (to obtain a typical Pc5 pulsation characterization), which allows us to do

a comparative analysis between regions. Additionally, the experimental period corresponds to data collected close to the equinox period to provide a better condition of an inter-hemispheric symmetry.

We search for comparison patterns of the Pc5 pulsations at conjugate stations to characterize the pulsations behaviors. To obtain a comprehensive investigation, we establish a methodology composed of several significant signal analysis techniques. First, the Fourier transform (Welch's power spectral) is performed to highlight the global scenario of the dataset, which allows examining the process among conjugate stations and their frequency characteristics. Second, a continuous wavelet transform is used for dealing with time-scale variability and regularity related to the local non-stationary aspects. Third, a wavelet coherence analysis grants us to find standard scales and evaluate the local similarity of Pc5 pulsations among conjugate stations. To the best of our knowledge, there has been no clear research combining this approach to analyze Pc5 pulsations and the role of the SAMA.

The content of this work is established as follows. Section 2 presents the data. Section 3 describes the signal analysis methodology. Section 4 shows and discusses the results. The last section summarizes the conclusions.

2 Data

In this section, we present the dataset used for this investigation, the ground-based stations considered, and the space environment conditions concerning the case study.

2.1 Geomagnetic Dataset

We use the geomagnetic horizontal (H) component recorded on the ground. This choice is because this component is more susceptible to the magnetosphere-ionosphere modulation effects. Therefore, this measurement is more suitable for the study of Pc5 pulsations in conjugate points [30, 48]. The record sampling rate is of seconds for all stations.

The data used concern the period between 09 : 00UT on 25 th and 21 : 00UT on 26 th October 2016, which corresponds to the main and recovery phases of a moderate geomagnetic storm ($Dst_{\min} = -52$ nT), which presented an abrupt magnetic increase (sometimes designated as SSC or SI) related to a magnetopause compression produced by a solar wind pressure pulse. We also calculated Pc5 pulsations corresponding to this period. Before 09 : 00UT on 25 th there were no significant Pc5 pulsations (Fig. 9, panel "h," in Appendix). Previous studies have shown that the largest Pc5 amplitudes are observed during such a kind of geomagnetically disturbed period [21, 34, 54]. Fortunately, the period of the storm was close to the September equinox, which ensures equal illumination by the Sun on both Earth's hemispheres. This condition creates inter-hemispheric symmetry and similarities both in conductivity and atmospheric electric current systems between the conjugate points [55, 56]. Those atmospheric characteristics enable dealing with a physical system somehow simplified. Information and discussion on space environment conditions for this selected data period are presented in Appendix.

2.2 Ground-Based Stations

To attend the investigation purposes, the selected stations are located at middle-to-low latitudes. Theoretically, they are close to the feet of the same magnetic field line (conjugate points).

In the first place, the best approach to finding conjugate points at low latitudes is to trace magnetic field lines in a geomagnetic model. The Magnetic Apex Coordinates [57] and Altitude adjustment corrected geomagnetic (AACGM) [58] could be used for most purposes. Both coordinates are defined using the IGRF at full resolution (for readers interested, they are available practically in the Python wrapper tool[1,2]. AACGM coordinates could be considered very similar to Modified Apex coordinates with reference height $h_R = 0$. To attend to our purpose, we choose AACGM coordinate representation because it is helpful for space weather. The AACGM coordinates are determined by following the magnetic field line from the geographic starting point to the magnetic dipole equator. The AACGM coordinates are then given by the latitude and longitude of the dipole field line that connects the point on the magnetic equator to the surface of the Earth. In this technique, all points on a given field line are magnetically connected and have the same AACGM coordinates [57]. The charged particles and pulsations are expected to follow trajectories along the field lines, so tracing them helps to understand how different regions of the ionosphere are coupled to one another, and this condition reflects a better magnetic conjugacy compromise. A user must pay attention to a forbidden region, which means an area where AACGM coordinates cannot be defined at low latitudes (around the magnetic equator). Sheperd and team [57] and Laundal and Richmond [58] consider in their studies this issue and present a figure that shows the region. However, with the updates of the AACGM and IGRF model, this region has become smaller in recent years than the one earlier calculated. We checked whether any stations used in this study fall in the forbidden region. Fortunately, none of the stations used in this study is within the forbidden region. Besides, for any practical user's purpose, the software

[1] https://pypi.org/project/aacgmv2/

[2] https://pypi.org/project/apexpy/

Table 1 Coordinates of the magnetic stations

	Stations		Coordinates					
			Geographic		Conjugate			
	Codes	Names	Lat	Lon	Lat	Lon	h_{eq}	L
			[°]	[°]	[°]	[°]	[km]	[R_E]
	KAK	Kakioka	36.23	140.18	-20.21	138.97	2417	1.47
	ASP	Alice Springs	-23.77	133.88	39.93	134.36		
Asia-Pacific	KNY	Kanoya	31.42	130.88	-15.94	130.99	1183	1.24
	KDU	Kakadu	-12.69	132.47	28.21	132.46		
	ABG	Alibag	18.62	72.87	-4.27	73.95	214	1.05
	GAN	Gan	0.69	73.15	13.83	72.60		
	DUR	Duronia	41.35	14.46	-24.14	18.79	3279	1.53
	KMH	Keetmanshoop	-26.54	18.11	43.03	12.46		
America-	SJG	San Juan	18.11	-66.15	-35.20	-55.06	1260	1.28
SAMA	SMS	São Martinho da Serra	-29.44	-53.82	14.38	-64.4		
	GUI	Guimar-Tenerife	28.32	-16.43	-4.33	-11.31	242	1.12
	ASC	Ascensio Island	-7.95	-14.38	21.67	-19.31		

mentioned can identify when the coordinates of a station fall in the forbidden region.

Here, the locations were obtained according to Altitude Adjusted Corrected Geomagnetic (AACGM) coordinates. This model uses the IGRF-13 to define the magnetic field line traces from one hemisphere to another, according to the procedure from [57]. AACGM model also allows the calculation of the maximum altitude h_{eq} of the magnetic line between the stations. Almost all stations used here belong to INTERMAGNET (International Real-time Magnetic Observatory Network)[3], except for the São Martinho da Serra station that belongs to Embrace network (Brazilian Study and Monitoring of Space Weather)[4] [59]. Related to the magnetic station locations, Table 1 presents the geographic and conjugate coordinates and L-shell values. Figure 1 shows the locations of the conjugate stations. Besides, the surface area of the SAMA is evidenced on the map by the closed (blue) line, provided by the magnitude isoline of 32,000 nT at the Earth's surface using the IGRF-13 model [2, 9, 11].

3 Methodology

We analyze the Pc5 pulsations by applying techniques such as spectral analysis. To obtain these Pc5 pulsations, we use a band-pass filter applied to the H component. Among the available filtering techniques, the infinite impulse response (IIR) band-pass filter [60, 61] has been selected because it provides the best performance. The band-pass filter frequency range was 1.6–7 mHz (frequency range of the Pc5), where the filtering obtains the best identification of the pulsations of interest.

3.1 Spectral Analysis

We performed our spectral analysis using two techniques: Time-Frequency analysis (based on Fourier transform) and Time-Scale analysis (based on a continuous wavelet transform).

Time-Frequency analysis is usually performed by a spectral decomposition of the signal using mathematical algorithms such as the Fourier transform (FT), which allows the decomposition of the signal in spectral components of high and low frequency. Mathematically, the fast Fourier transform decomposes any signal into a sum of sinusoids and transforms each into the frequency domain. This spectral analysis provides a complete description of the frequency content of a given time series [62].

It is well known that for a finite length record of data, the finite FT is given by:

$$F(\xi) = \int_0^T f(t) e^{-2\pi\imath\xi t}\, \mathrm{d}t\,, \tag{1}$$

where T is the record length, ξ is the frequency, and $x(t)$ is the time series from which we extract the record of length T, in our case a Pc5 pulsation time series.

In this analysis, we used Welch's power spectral density, using the fast FT (FFT) analysis, so that the spectral features could be more clearly identified in the frequency range of

[3] www.intermagnet.org/index-eng.php

[4] www2.inpe.br/climaespacial/portal/en/

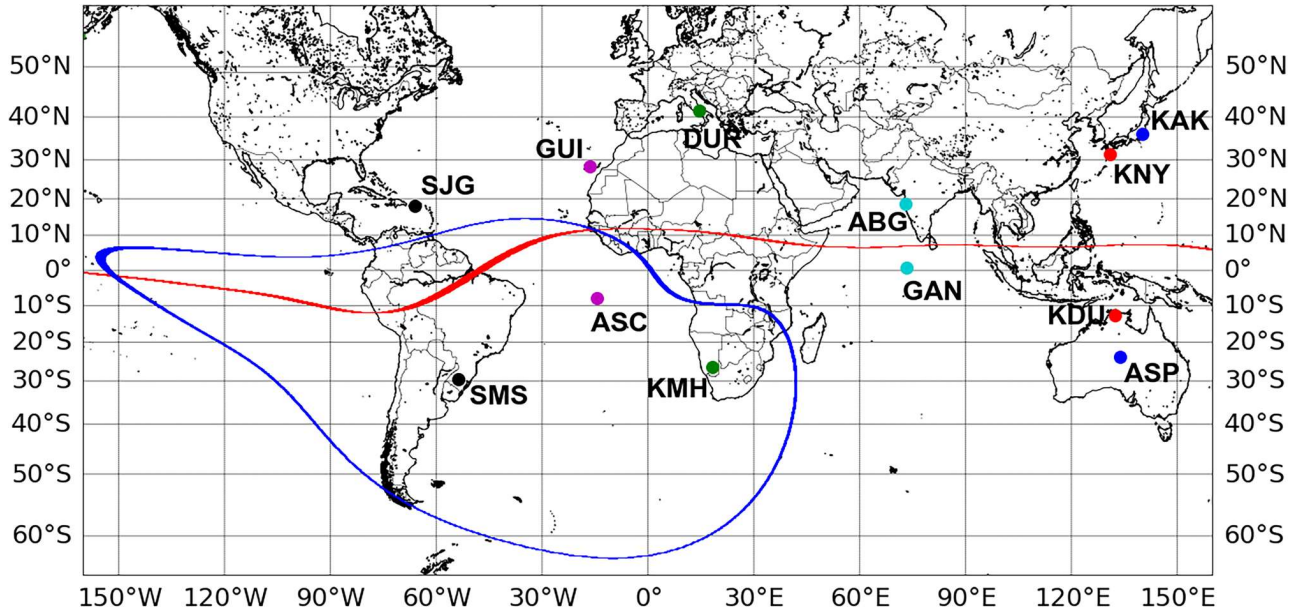

Fig. 1 Map of conjugate stations, indicated by circles. The line (in red) crossing the map is the dip equator and the closed line (in blue) surrounds the SAMA region

interest. A Hanning window of length 64 s was applied to the data in the time domain.

For time-scale analysis, we compute the wavelet coefficients $\mathcal{W}_f^{\psi}(a,\tau)$ obtained from the continuous wavelet transform (CWT) of the Pc5 pulsations $f(t)$ defined by:

$$\mathcal{W}_f^{\psi}(a,\tau) = \frac{1}{\sqrt{a}} \int_{-\infty}^{\infty} f(t)\, \overline{\psi(\frac{t-\tau}{a})}\, \mathrm{d}t \qquad a > 0\,, \tag{2}$$

where a is scale, τ denotes translation, and $\overline{\psi}$ is a complex conjugate of the analyzing wavelet function, ψ [63, 64]. The analyzing wavelet function used in this work is the Morlet function defined by:

$$\psi(t) = \pi^{-\frac{1}{4}}\ \exp(\imath 5\, t)\ \exp\left(-\frac{t^2}{2}\right). \tag{3}$$

In essence, the CWT can be used to decompose a complicated wave-like signal in its scale components (central-periods components). The advantage of CWT analysis is that it is suitable for studying non-stationary, nonlinear signals, as geophysics signals, and provides information not only about the central-frequencies (inverse of central periods) of the events, but also about their location in time. From using the CWT technique, the square modulus of the wavelet coefficients is computed, creating a signal energy representation per scale per time, usually designated as scalogram. In summary, the scalogram can be understood as the signal energy distribution in time τ and scale a.

3.2 Coherence Analysis

In principle, coherence analysis can quantify any probable (co-relational) relationship between signals [65, 66]. This part of the methodology evaluates if the Pc5 pulsations are coming practically from the same source region, i.e., if they are observed simultaneously at the conjugate stations. Any dissimilarity can also identify disturbances caused both by locally morphological processes and asymmetrical effects from external sources.

The cross wavelet transform is a wavelet analysis tool that enables us to deal with the Time-Scale dependencies between two time series, defined as:

$$\mathcal{W}_{f,g}^{\psi}(a,\tau) = \mathcal{W}_f^{\psi}(a,\tau)\ \mathcal{W}_g^{\psi}(a,\tau), \tag{4}$$

where $\mathcal{W}_f^{\psi}(a,\tau)$ indicates the wavelet transform of the signal $f(t)$, and respectively $\mathcal{W}_g^{\psi}(a,\tau)$ the signal $g(t)$ [67–69].

Based on this cross-transform, we can compute the wavelet coherence $\mathcal{C}_{\mathcal{W}}^2(a,\tau)$ and a phase measure. They provide linear-quantitative estimators of the degree the relationship by scales between the two signals [69, 70]. Here, the wavelet coherence is computed using the following expression:

$$\mathcal{C}_{\mathcal{W}}^2(a,\tau) = \frac{|S(a^{-1}\mathcal{W}_{f,g}^{\psi}(a,\tau))|^2}{S(a^{-1}|\mathcal{W}_f^{\psi}(a,\tau)|^2)\ S(a^{-1}|\mathcal{W}_g^{\psi}(a,\tau)|^2)} \tag{5}$$

where $\mathcal{C}_{\mathcal{W}}^2(a,\tau)$, as defined, ranges between 0 and 1, and S is a smooth operator in Time-Scale domain. We adopted

the operator S as a convolution of the transform coefficients with a smoothing Gaussian moving average, in both time and scale directions [68]. This smoothing process is used to avoid unnecessary noise due to the amplification provided by the product. We plot these coefficients in a colormap graph similar to the scalogram used in the wavelet transform.

As stated earlier, the coherence helps us to determine whether the Pc5 pulsations come from the same source region in the frequency domain. When $\mathcal{C}^2_{\mathcal{W}}(a,\tau)$ equals 0, the two signals do not correlate, indicating that these two signals are coming from two different sources or significantly altered source conditions. On the other hand, if the $\mathcal{C}^2_{\mathcal{W}}(a,\tau)$ is close to 1, with the same frequencies between two signals, the two signals are identical, indicating that these two signals are coming from the same source condition region [71, 72].

The wavelet coherence phase $\theta_{x,y}$, here called just as phase, is obtained by the real and imaginary coefficients:

$$\theta = \tan^{-1}\left(\frac{\mathfrak{I}\left\{S(a^{-1}\mathcal{W}^{\psi}_{f,g}(a,\tau))\right\}}{\Re\left\{S(a^{-1}\mathcal{W}^{\psi}_{f,g}(a,\tau))\right\}}\right). \tag{6}$$

This measurement yields information on the delay of one signal considering the other as a function of time and scale.

4 Results and Discussions

For both regions of the globe, the results concern the Pc5 event identification, the power spectral density analysis, the wavelet analysis aiming at process dynamics, the signal-conjugate coherence analysis, and at last comparison of the behaviors affected by the SAMA and outside.

4.1 Pc5-Event Identifications

Initially, we recall that interplanetary phenomena as composed of a solar wind plasma incident upon the Earth establish, according to the direction of the interplanetary magnetic field carried in the plasma, electrodynamical processes transferring energy and momentum. As one external source of Pc5 magnetic pulsations, a solar plasma laminar flow creates in the magnetopause flanks Kelvin-Helmholtz instabilities. Those instabilities generate Pc5 magnetic pulsation by means of Alfvén waves propagating in the geomagnetic field towards their edges on the terrestrial surface. Those pulsations can be recorded on the ground from middle to high latitudes. As another cause, an enhanced solar wind plasma can produce abrupt magnetosphere compression increasing electrical currents in the frontal magnetopause. This compression followed by or during a decrease of the geomagnetic field is expected to trigger and develop Pc5 pulsations from middle to low latitudes ($\leq 45^o$). Also, internal causes such as field Line Resonance and cavity/waveguide modes have been proposed as mechanisms able to modify magnetic pulsations evolving in dipolar field lines in the middle to low latitudes.

Using Fig. 9, panels "*d*" and "*h*" (in Appendix), we verified Pc5 pulsations in Kakioka station at middle latitude (36.23°N) developed when a moderate geomagnetic storm started about 04 : 00UT October 23 th 2016. The low-magnitude Pc5-pulsation episodes can be seen related to small pulses in solar plasma pressure in the figure. Vertical lines indicated by letters A, B, and C, indicate compression examples (panel "*d*") and the respective Pc5 pulsations triggered (panel h). When there is an intense pressure pulse at about 09 : 20UT, October 25 th, significant Pc5 pulsations start. Pc5 pulsations are recorded in all selected stations. We have noticed the maintenance of those intense pulsations at middle to low latitudes is connected to a significant magnitude of geomagnetic storm development.

Prepared according to the filtering treatment, Fig. 2 shows the Pc5 pulsations of each conjugate pair in both regions. Each pair indicated by superior (in red) and inferior (in blue) signals is presented from top to bottom. We initially chose five time intervals representing simultaneous wave packs of Pc5 pulsations. These intervals were chosen considering the larger Pc5-pulsation amplitudes in both regions (seen in this figure) and the significant wavelet coefficients (seen in Figs. 5 and 6, later described), during the geomagnetic storm.

4.1.1 Asia-Pacific Region

Through a visual inspection in this figure, the first three panels from the top (i.e., plots a, b, and c) concerning the Asia-Pacific region reveal typical Pc5-pulsation evolution patterns. Pc5 wave packets occur simultaneously and similarly between the conjugate stations, composing a behavior which reinforces the information reported in previous studies about conjugate stations, such as [30, 39, 46, 73, 74]. Showed clearly in the first three time intervals and last one (i.e., intervals 1, 2, and 3, and 5), Pc5-pulsation amplitudes present a systematic decrease with decreasing latitude or L-shell ($\mathrm{Pc5}^{\mathrm{L=1.05}}_{\mathrm{ABG\text{-}GAN}} < \mathrm{Pc5}^{\mathrm{L=1.24}}_{\mathrm{KNY\text{-}KDU}} < \mathrm{Pc5}^{\mathrm{L=1.47}}_{\mathrm{KAK\text{-}ASP}}$), in accordance with [54, 75, 76]. Moreover, it is significant to clarify that these previous studies did not work with conjugate stations; we adopted this methodological procedure in our work.

In particular, intervals 1 and 2 highlight after an abrupt H-component increase (due to magnetopause compression), and the Pc5 pulsations are intensified. The pulsation amplitudes are noticed to increase associated with an intensification of the magnetic disturbance

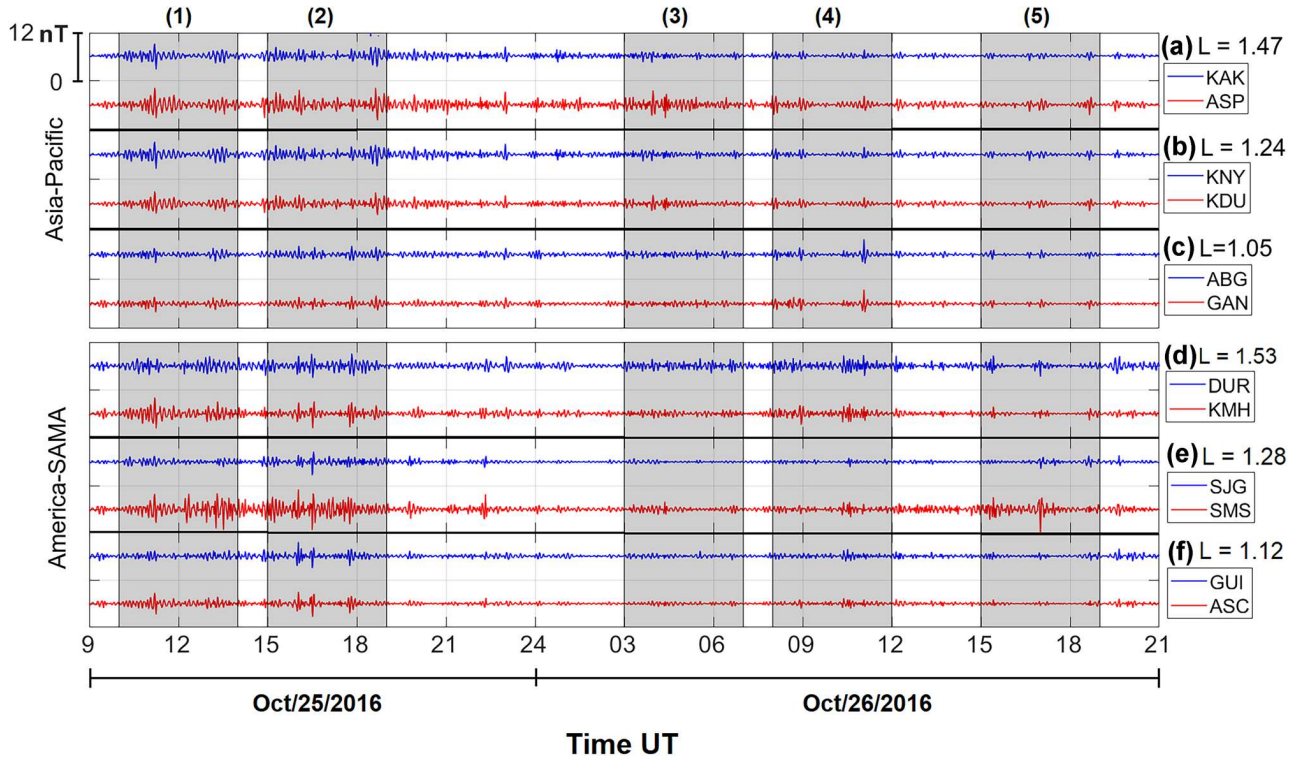

Fig. 2 Filtered Pc5 pulsations at conjugate stations. **a** KAK-ASP, **b** KNY-KDU, **c** ABG-GAN, **d** DUR-KMH, **e** SGJ-SMS, and **f** GUI-ASC

at the ground reaching lower values ($Dst \leq -30$ nT) and becoming a moderate geomagnetic storm (-100 nT $\leq Dst_{min} < -50$ nT). In the conjugate stations, pulsation amplitudes decrease with the decreasing of station latitudes due to physical mechanisms in the ionosphere. The pulsation damping rates are strongly dependent on the ionospheric conductivity, as expected according to discussed in [77], the higher electrical conductivity, the taller wave damping. Thus, from the plot c, Pc5 pulsations present intense damping for stations near the magnetic equator, agreeing with the evaluation done by [78] and [22], which state that this location presents the highest Cowling conductivity value.

Furthermore, for L-shell values less than 1.5, the magnetic line is inside the plasmasphere-ionosphere system (see Table 1). Therefore, both field line oscillations and pulsations can be strongly dampened, which is consistent with some previous investigations, for instance [77, 79]. It is worth mentioning that the damping for the ABG-GAN conjugate pair is more intense because the magnetic line is entirely within the ionosphere (altitude $h_{eq} \sim 200$ km). This fact implies that Pc5 should be more damped, and this effect depends predominantly on conductivity (Pedersen and Hall) [22, 79, 80].

4.1.2 America-SAMA Region

It is noticed from the last three panels at the bottom (d, e, and f) in Fig. 2 that Pc5 wave packets in the southern hemisphere are, in general, more intense in amplitude than the pulsations in the northern hemisphere concerning the conjugate pairs. Mainly, paying attention to the SJG-SMS pair, SMS presents the largest pulsation during the main phase. With the GUI-ASC pair, their pulsation amplitudes are more in harmony, but with the smallest amplitudes. On the one hand, only in the northern hemisphere do the Pc5 amplitudes show a systematic decrease associated with the latitude or L-shell reductions, as reported for the Asia-Pacific region. On the other hand, immediately after a sudden magnetic impulse, there is an enhancement of Pc5 pulsation amplitudes at a location close to the SAMA center compared to other stations further away in this South American region, as mentioned by [81, 82].

In the northern hemisphere, pulsation amplitude decrease associated with the latitude in a typical way. During the geomagnetic storm main phase, in the SAMA region, an enhancement of Pc5-pulsation amplitude occurs, which may be associated with electron precipitation into the ionospheric D and E layers. Situated near the SAMA center, SMS

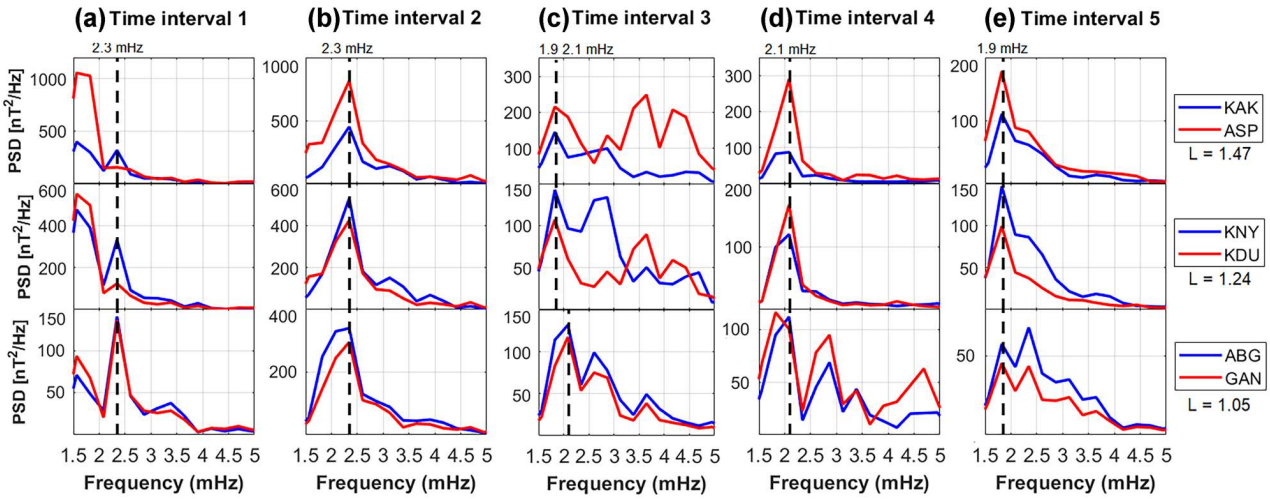

Fig. 3 Welch's power spectral density of the Pc5 pulsations from conjugate station in the Asia-Pacific region: time interval 1 (**a**), 2 (**b**), 3 (**c**), 4 (**d**), and 5 (**e**)

presented the highest pulsation amplitude, KMH located close to the secondary anomaly valley showed the second intense amplitude, and ASC seemed to follow the typical behavior of its conjugate station.

4.2 Pc5 Power-Spectral Density Analysis

Here, we use a power spectral technique to investigate the prominent peaks and the similarity between the conjugate-station pairs.

4.2.1 Asia-Pacific Region

Figure 3 shows Welch's power spectral density (PSD), obtained from FFT, applied to the filtered time series for the selected intervals.

The figure shows the intensity of frequency contributions to the Pc5 pulsations occurring in all intervals for the conjugate pairs. In intervals 1 and 2, a significant discrete spectral peak is shown for each conjugate pair at 2.3 mHz. In interval 3, the significant peaks are close, at 1.9 and 2.1 mHz. In intervals 4 and 5, the significant peaks are observed simultaneously at 2.1 and 1.9 mHz, respectively. Those dominant frequencies found (2.3, 2.1, and 1.9 mHz) are pretty consistent with some of the discrete peaks observed at low latitudes by [83–86]. One can notice from the PSD the higher values in the main phase and the intensity decreasing in the recovery phase. Also, the PSD intensities decrease towards the magnetic equator (i.e., panels from top to bottom in the figure). The PSD results highlight a decrease in amplitudes with the reduction of latitudes, following a pulsation behavior similar to driven by an external source. The higher PSD values follow, in a general sense, the decrease in the intensity from the main phase towards the recovery phase.

4.2.2 America-SAMA Region

Figure 4 shows Welch's PSD calculated to the America-SAMA region.

In time interval 1, two discrete spectral peaks around 1.9 mHz to the pairs DUR-KMH and SJG-SMS and 2.3 mHz practically to all are shown. SMS presents a significant peak of about 2.8 mHz, which is suggested in the other Southern stations. In interval 2, a discrete spectral peak of 2.1 mHz is shown for the DUR-KMH stations and another in 2.6 mHz for GUI-ASC stations. To pair SJG-SMS, there are peaks of about 2.8 and 3.2 mHz, with strong intensities for SMS station, which presented a peak in 2.3 mHz. In intervals 3 and 5, a peak of about 1.9 mHz appears in almost all stations, except in SJG. Lastly, there is a significant peak at 2.8 mHz in interval 4. While the GUI-ASC and DUR-KMH seem to follow the Asian-Pacific pair behavior, SJG-SMS is very discrepant. Most of dominant frequencies found (2.8, 2.6, 2.3, 2.1, and 1.9 mHz) are quite consistent with the earlier studies, reinforcing researches such as done by [83, 84, 86]. However, their studies were conducted outside of the anomaly.

One can notice the higher PSD values do not follow, in a general sense, the decrease in the intensity concerning the main phase and the recovery phase, maybe except by pair GUI-ASC far away from the magnetic (main and secondary) anomalies. Also, the conjugate stations affected by the SAMA do not obey the PSD amplitudes decreasing with the decrease in latitudes. Moreover, it is important to remember that the particle precipitation is not symmetric in the SAMA

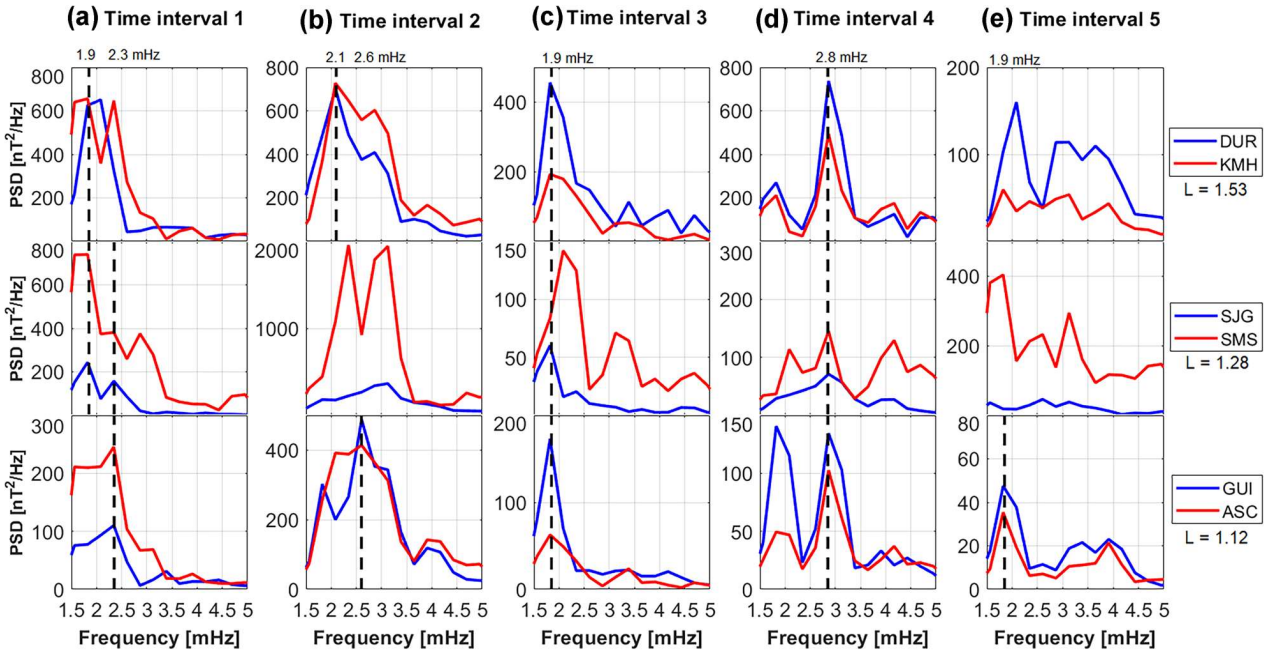

Fig. 4 Welch's power spectral density of the Pc5 pulsations from conjugate station in the America-SAMA region: time interval 1 (**a**), 2 (**b**), 3 (**c**), 4 (**d**), and 5 (**e**)

region, as pointed out by [87]. Those PSD results highlight that the typical magnetosphere effects, as considered by [85], are influenced by an altered upper atmosphere in the SAMA region, mainly by the ionosphere.

4.3 Wavelet Analysis of Pc5 Dynamics

Here, we analyze the signal energy per scale along the time (Figs. 5 and 6). A plot designated scalogram helps to visualize the maximum value location and their temporal occurrence and provides an efficient approach to examining pulsation details highlighting similarities.

4.3.1 Asia-Pacific Region

For the Asia-Pacific region, Fig. 5 shows the Pc5 pulsation signal (at the top) and the respective scalogram (at the bottom) together at each panel concerning each station. The horizontal axis represents time in hours, and each vertical axis represents respectively the signal intensity (in nT) and the wavelet scale (in mHz). The wavelet coefficient magnitudes are indicated according to the color bar, which has the same range (nT^2/mHz) for the signal analysis of each station. The panels in the same vertical column present the stations (at left) for the Northern hemisphere and (right) for the Southern one, while the panels in the same horizontal position refer to the conjugate station pairs.

The figure highlights the detail in the Pc5 pulsations. The maximum values of wavelet coefficients (yellow color, top in the color bar) coincide with the most intense Pc5 wave packets exhibited at each station.

In the first two time intervals, during the main phase, the scalograms show the main spectra between frequencies 1.6 and 4 mHz. The wavelet coefficients present more intense values in the pairs KAK-ASP and KNY-KDU. In the third interval, starting the recovery phase, the main frequencies are between 1.6 and 7 mHz. The coefficients are observed with a little intensification in the southern hemisphere stations such as ASP and KDU. In the fourth interval, the main frequencies are between 2 and 5 mHz. The coefficients are observed with greater intensity in the ABG-GAN conjugate stations, located close to the magnetic equator. In the fifth interval, the intensities are reduced. The slight differences in the scalograms may be credited to subtle ionospheric currents and local features of each conjugate station. A higher similarity of the scalograms can be observed initially using the same hemispheres: KAK and KNY (in the northern), ASP and KDU (in the southern), and later comparing the hemispheres. This similarity in the scalograms of the mentioned stations may be because the stations (of each hemisphere) are relatively close.

The scalogram inspection reveals similar features in energy amplitude, duration, and scale (converted to central frequency) for the conjugate pairs. From the similar energy patterns detected, we can conclude the conjugate pairs in

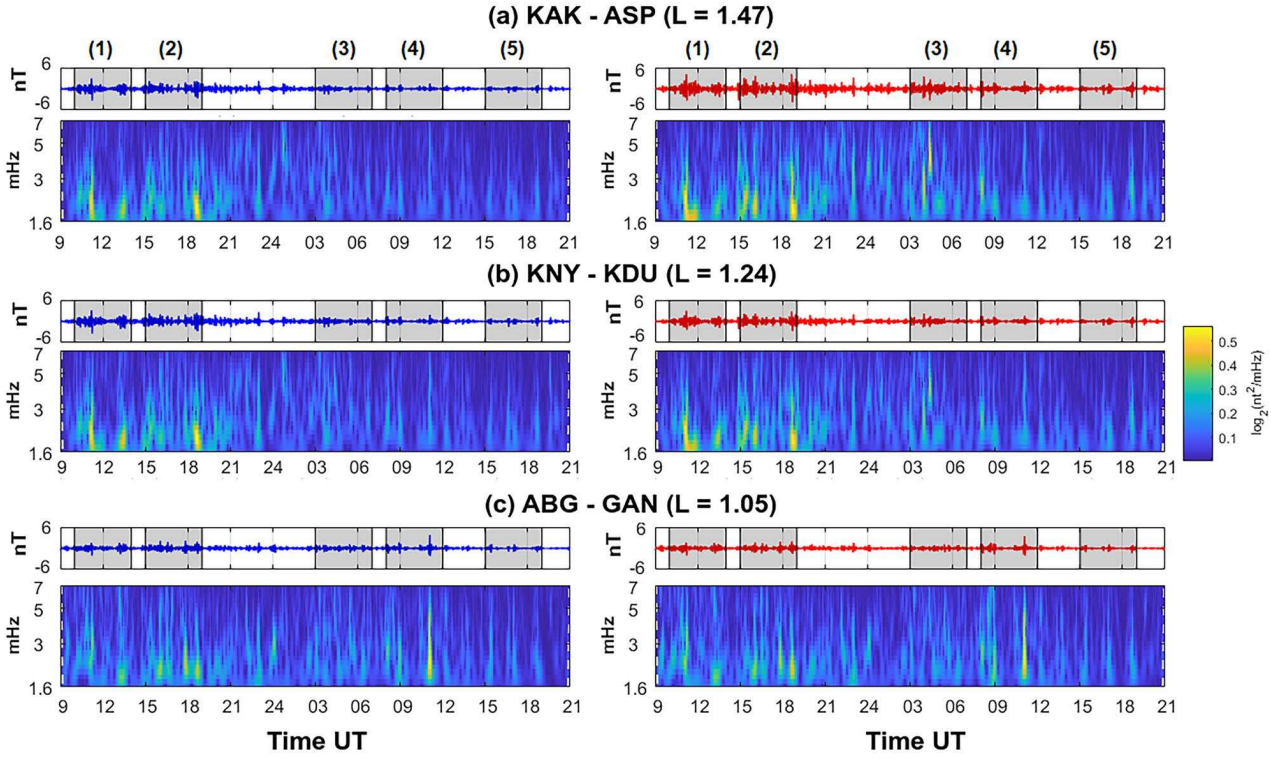

Fig. 5 Pc5 pulsations (top) and squared-wavelet coefficients–scalograms (bottom) for each pair of conjugate stations: **a** KAK-ASP, **b** KNY-KDU, and **c** ABG-GAN

Asia-Pacific are subject to practically the same magnetosphere-ionosphere system conditions.

4.3.2 America-SAMA Region

Figure 6 shows the Pc5 pulsation signal and the respective scalogram together (top and bottom panels, respectively) for each station, in a similar way of the earlier figure, but concerning the America-SAMA region.

The scalograms show the most intense Pc5 pulsations in the first two time intervals, which correspond to the main phase of the magnetic storm. We can verify that the primary spectra are between frequencies 1.6 and 5 mHz. The wavelet coefficients present higher values in the pair DUR-KMH and SJG-SMS. In the third interval, starting the recovery phase, the wavelet coefficients present reduced values, except in DUR. In the fourth interval, the pair DUR-KMH shows wavelet coefficients with slightly higher values than the others. In the fifth interval, close to a little magnetic decreasing during the recovery phase, the station SMS present significant values, particularly about 1.9–3.5 mHz.

Initially, from the scalograms, we can notice a typical pattern for the Southern stations, particularly the wavelet coefficients with the higher energy during the main phase. A decrease in the magnetic field during a storm seems to be related to an intensification of the Pc5 pulsation. Considering the stations SMS, close to the primary SAMA center, and KMH, close to a secondary minimum, we can notice intense pulsations and similarity in the energy patterns. Station DUR in the Northern hemisphere seems to follow the Asian-Pacific energy pattern, while SJG and GUI also in the Northern have energy patterns with more reduced coefficient values. The high-latitude pair DUR-KMH seems sensitive to an external source, as expected of a magnetic line interlinking outside the ionosphere. The other stations, not considering here SMS, present low L-shell behavior (or low latitude) because the magnetic flux lines are inside the ionosphere (see Table 1).

We recall we are dealing with phenomena occurring close to a period of almost inter-hemispheric illumination symmetry because of the time proximity with the September equinox. Stations of Asian-Pacific are under symmetric conditions (magnetopause causes, plasmasphere and ionosphere conditions, and symmetric adjacent L-shells). Stations of America-SAMA are under the same magnetopause causes, the stations are not under symmetric particle precipitation nor plasmasphere-ionosphere L-shells symmetry, and the pair SJG-SMS is subjected to the South America peculiarities of the equatorial ionization anomaly. The SAMA ionization is treated in detail in [87] and the ionization anomaly

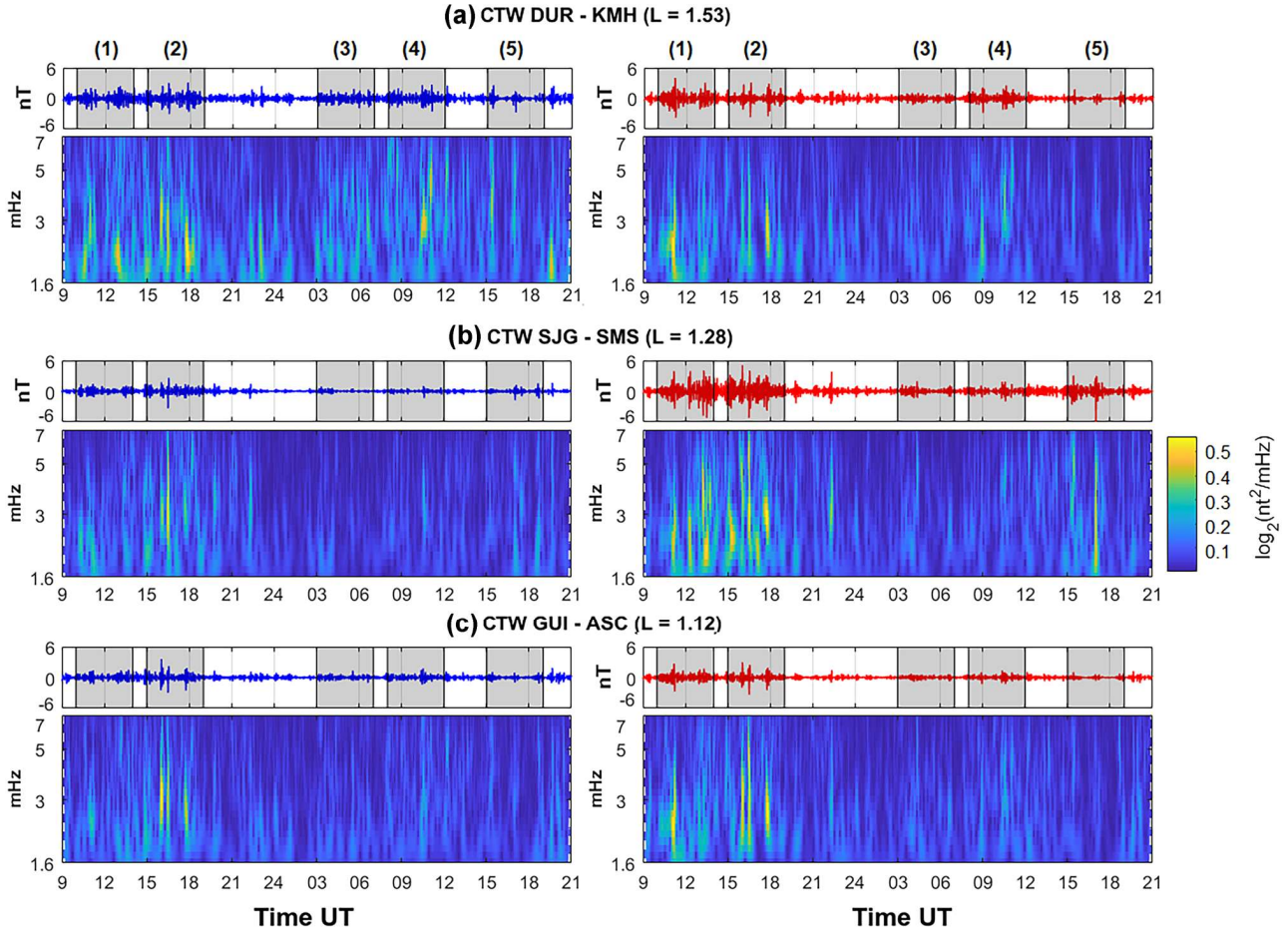

Fig. 6 Pc5 pulsations (top) and squared-wavelet coefficients–scalograms (bottom) for each pair of conjugate stations: **a** DUR-KMH and **b** SJG-SMS, **c** GUI-ASC

in [88, 89]. Our work could not discuss internal causes of Pc5 pulsations (such as FLR or cavity/waveguide mode), which demand other kinds of data; that way, only external causes can be appreciated by us. That way, the Pc5 pulsation mechanisms connected to an inner-magnetosphere, plasmasphere, and ionosphere system and their interacting dynamics remain to be explained adequately in future. Nevertheless, the results show that the SAMA affects the Pc5 pulsation occurrence. The CTW technique to investigate time-scale characteristics has significantly aided this work. The simultaneous Pc5 pulsations in a long-lasting geomagnetic storm, about 36 h (in universal time), eliminate the hypothesis of an exclusive local-time effect.

4.4 Coherence Analysis

To complete the investigation, we use the coherence analysis to clarify the following question: *Given a pair of signals from conjugate stations, how similar are the power spectral of these signals*?

Calculated by Eq. 5, the wavelet coherence result for each conjugate pair in both globe regions allows for building a colormap plot (Figs. 7 and 8). The colors represent the coherence values of Pc5 pulsations between the conjugate pair. The yellow color (top in the color bar) indicates a value around 1, which is the maximum wavelet coherence between the Pc5. Arrows indicate the phase (given by Eq. 6) between the signals. In-phase is the right arrow, the anti-phase is to left, and the inclined arrow gives intermediate values. For a convenient visualization, arrows are shown only where the coherence is larger than or equal to 0.8.

4.4.1 Asia-Pacific Region

As seen in Fig.7, time intervals for Asia-Pacific stations show practically high coherence and in-phase signals for pulsations in the conjugate stations. In a detailed inspection, intervals 1, 2, and 3 show that both values increased with decreasing L-shell (or latitude). Coherence results, by wavelet representation, show the stations (ABG-GAN), which has

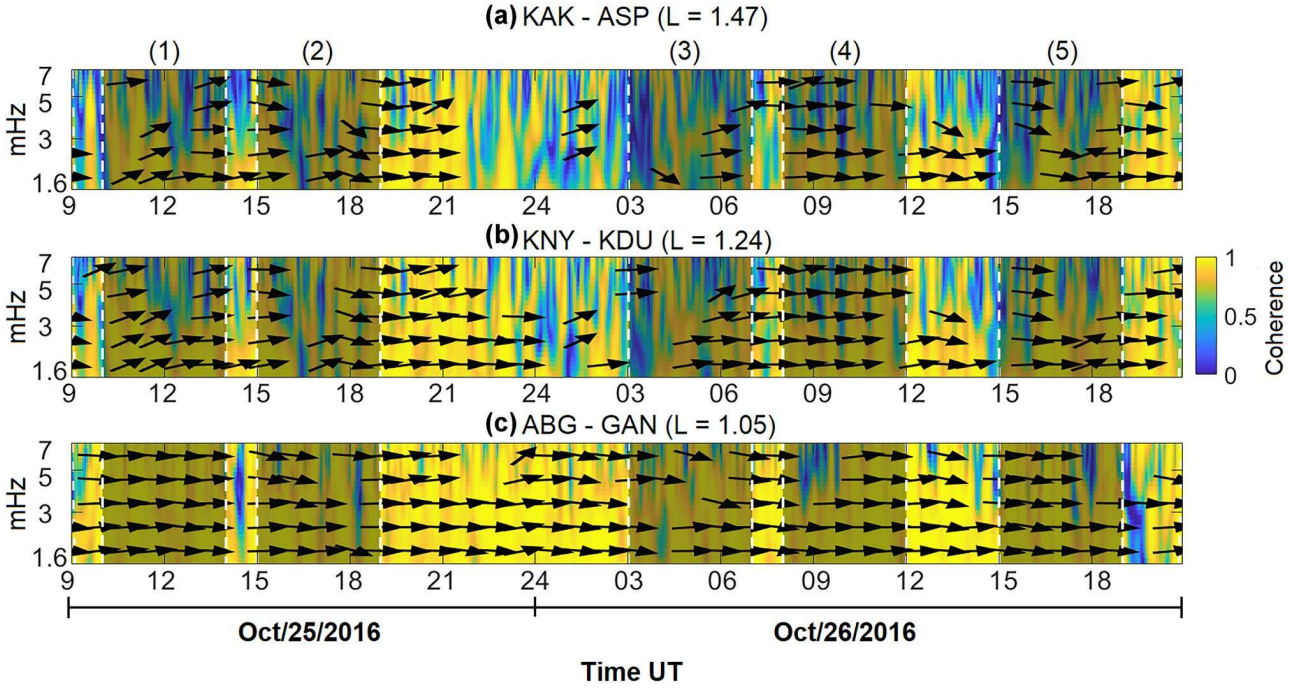

Fig. 7 Wavelet coherence representations for Pc5 pulsations between the conjugate pair stations. Color map indicates the amplitude, and arrows the phase where the amplitude is larger than 0.8. **a** KAK-ASP, **b** KNY-KDU, **c** ABG-GAN

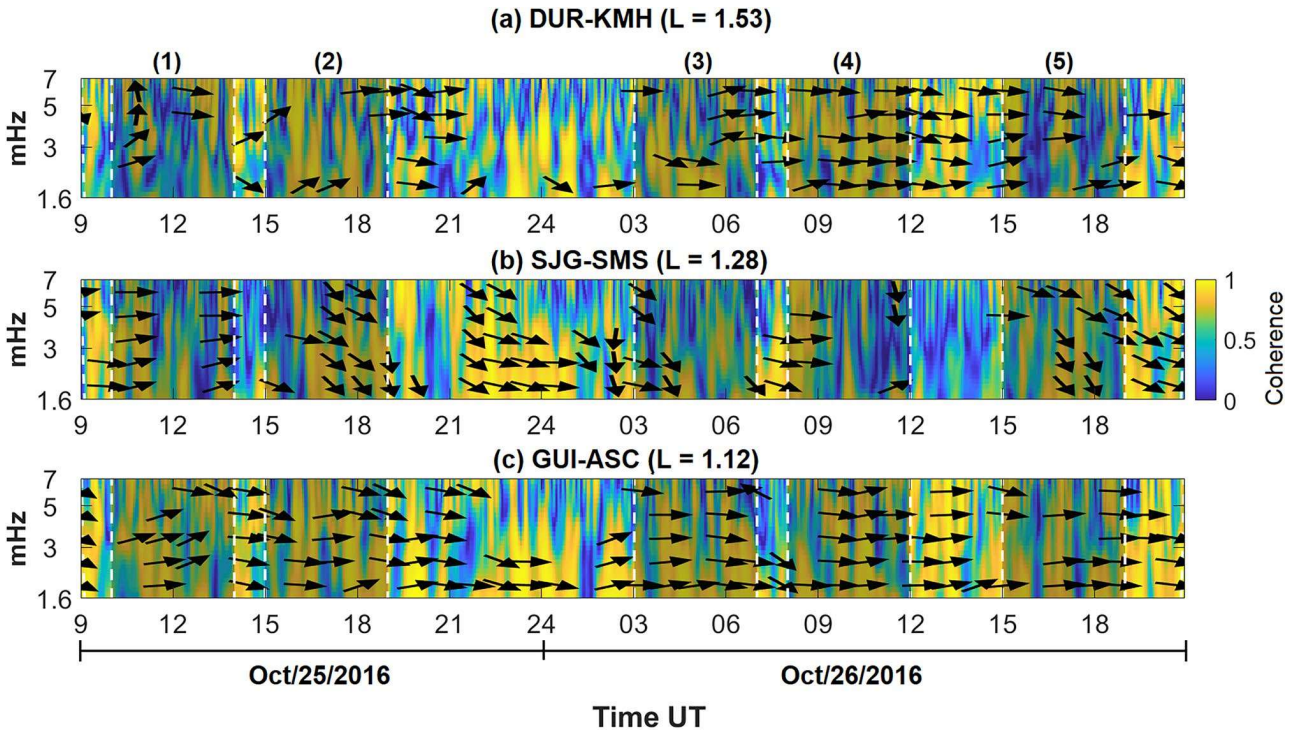

Fig. 8 Wavelet coherence representations for Pc5 pulsations between the conjugate pair stations. Color map indicates the amplitude, and arrows the phase where the amplitude is larger than 0.7. **a** DUR-KMH, **b** SJG-SMS, and **c** GUI-ASC

the lowest L-shell value, as the most coherent. In contrast, the pair KAK-ASP, which has the highest values of L-shell and h_{eq}, shows the lowest coherence. These results show the stations are subjected to similar effects and similarly developed processes.

4.4.2 America-SAMA Region

Figure 8 shows the wavelet coherence result for each conjugate pair in the America-SAMA region. By examining the time intervals, there is generally less coherence and the highest variation in the phases between the pulsations. The GUI-ASC conjugate pair, with the lowest h_{eq} (or L-shell) value, appears as the most coherent among the conjugate-station pairs (seen in intervals 1, 2, 3, and 5). On the other hand, the pair SJG-SMS has the least coherence (seen in intervals 1, 3, 4, and 5). For this region, the coherence examination allows us to conclude, considering a general pattern, that their values do not increase with the decrease of the L-shell (or latitude).

As seen in this figure, arrows help us to interpret the phase lag between the conjugate pair signals. The pair GUI-ASC presents prevalent arrows point right, i.e., in phase. Following, the pair DUR-KMH presents some intervals (1, 2, and 3) with a slight displacement of the signal phase. At last, the pair SJG-SMS presents strong phase variation in some intervals (2, 3, 4, and 5), where almost vertical arrows indicate a $\pi/2$ or quarter-cycle (quadrature) phase lag between SMS and SJG.

In a detailed examination, the pair GUI-ASC presents the magnetic line crossing the lowest altitude considering the maximum altitudes of the magnetic line seen in Table 1 in this case $h_{eq} \sim 242$ km (or L-shell ~ 1.12). This line traverses the lower ionosphere. Furthermore, these stations present Pc5 pulsations with moderate coherence (between 0.4 and 0.7) in almost all intervals, and they also have the most damped amplitudes (Fig. 2, panel f). In the second place, SJG-SMS stations show weak coherence ($0.2 < C_{xy} < 0.4$). The corresponding magnetic line reaches the altitude $h_{eq} \sim 1260$ km (or L-shell (~ 1.28), which implies that the line that interlinks the two conjugate stations is inside the ionosphere. The weak pulsation coherence between this pair could be because the SMS station is close to the SAMA center. In this region, pulsations have been modified. The enhancement of Pc5 amplitudes and phase lag at SMS, in a location close to the SAMA center, could be attributed to precipitation of particles besides increased ionospheric conductivity gradients due to ionization rate in the D and E layers. At last, the pair DUR-KMH has the highest magnetic line altitude ($h_{eq} \sim 3279$ km, or L-shell ~ 1.53). This line traverses the ionosphere and reaches the plasmasphere.

From the results, Pc5 pulsations in the America-SAMA generally showed phase lags and moderate to low signal coherence. Thus, if the wave structures come from the same source regions, the SAMA magnetic morphology and the magnetic decrease due to the magnetic storm involving particle precipitation and electrical conductivity alteration modify undoubtedly plasmasphere-ionosphere system conditions. The system conditions affect the Pc5 pulsations structured in the magnetic line interlinking conjugate stations.

4.5 Pc5 Pulsations Inside SAMA and Outside: Scenario

In this investigation developed as a case study, the cause of the Pc5 pulsations is a triggering due to magnetopause compression produced by a significant solar wind plasma enhancement and the pulsation-amplitude maintenance is connected to the geomagnetic storm development. The pulsations effects were recorded by all middle-to-low-latitude conjugate magnetic-station pairs located in two broad regions; one of these regions is under the SAMA influence. Those Pc5 pulsations occur conveniently close to a period of interhemispheric illumination symmetry because of the time proximity with the September equinox, which mitigates the complexity of the geophysics processes involved.

Pc5 pulsations occur simultaneously and similarly between the conjugate stations in the Asia-Pacific region. Pc5-pulsation amplitudes present a systematic decrease with decreasing latitude or L-shell. The pulsation amplitude damping is strongly dependent on the ionospheric conductivity. The pulsation source corresponds to the magnetopause compression mechanism, which affects the magnetic lines and produces Pc5 pulsation. The higher amplitudes correspond to a higher exposition in altitude (understood in L-shell) of the magnetic field interlinking the conjugate pairs. The field paths sometimes cross the plasmasphere beyond the ionosphere.

Concerning the America-SAMA region, the Pc5 pulsation amplitudes in the Northern hemisphere stations presented pulsation amplitudes following the Asia-Pacific amplitude behavior. However, in the SAMA region, an enhancement of Pc5-pulsation amplitude recorded in the stations occurs associated with probable electron precipitation into the higher ionosphere. Situated near the center of SAMA, SMS presented the highest pulsation amplitude, KMH located close to an anomaly secondary minimum showed the second intense amplitude, and ASC seemed to follow the typical behavior of its conjugate pair. The higher amplitudes occur during the main phase of the geomagnetic storm or in the recovery phase when there is a significant magnetic decrease.

The dominant frequencies (1.9, 2.1, and 2.3 mHz) found in the Asia-Pacific region showed a pretty consistent way with the values observed at low latitudes in previous studies. The PSD results verified a decrease in the signal

intensity with the reduction of latitudes following a pulsation behavior similar to driven by an external magnetospheric source. In the America-SAMA region, although dominant frequencies (1.9, 2.1, 2.3, 2.6, and 2.8 mHz) are in accordance with the other globe region pattern, the PSD-intensity results do not follow the decrease in the intensity concerning the main and recovery storm phases. This behavior difference in PSD-intensity confirms the conjugate stations affected by the SAMA, in which the upper atmosphere, mainly the ionosphere, is altered concerning symmetric conditions.

Investigating the Pc5-pulsation dynamics during the geomagnetic storm period, the conjugate pairs in Asia-Pacific present energy patterns subjected to quite similar magnetosphere system conditions. Nevertheless, the America-SAMA conjugate pairs reveal a complicated pulsation pattern. The pulsation energies associated with the wavelet coefficients are highest during the main phase of the geomagnetic storm. We can notice intense pulsations and similarities in the energy pattern of the SMS and KMH, close respectively to SAMA primary and secondary magnetic minima. At the same time, station DUR in the Northern hemisphere seems to follow the Asia-Pacific energy pattern. We could claim attention to stations of the Asia-Pacific region under symmetric conditions (magnetopause causes, plasmasphere and ionosphere conditions, and symmetric adjacent layers, i.e., L-shells). In contrast, stations in the pairs in the America-SAMA are not under symmetric conditions. Those pairs are under the similar magnetopause causes; however, they are not under symmetric particle precipitation nor plasmasphere-ionosphere L-shell symmetry, and the pair SJG-SMS is subjected to the equatorial ionization anomaly. Those aspects corroborate the conclusion that the SAMA affects the Pc5 pulsation occurrences. Out of its current scope, this work does not discuss internal causes of magnetic pulsation modifications. Efforts with this purpose require examining extensive data from a net of ground equipment to study the ionosphere and even satellites to probe the plasmasphere.

At last, to complete the physical scenario concerning the middle-to-low latitude Pc5 pulsations, coherence analysis technique results identified that Pc5 pulsations in the Asia-Pacific region show high signal coherence and in-phase signals. Those values increased with decreasing L-shell (or latitude). In the America-SAMA region, Pc5 pulsations showed moderate to low coherence and phase lags between the signals. We can consider that if the Pc5 wave structures result similarly from the same external source, these structures can be affected by the magnetic morphology of SAMA, particle precipitation due to magnetic decrease during a magnetic storm, and involved electrical conductivity alterations. Those plasmasphere-ionosphere (no more symmetrical) system conditions affect the Pc5 pulsations in the magnetic line, which interlinks conjugate stations in the America-SAMA region, under conditions differing substantially from the Asia-Pacific one.

5 Conclusion

We investigated middle-to-low latitude Pc5 pulsations using geomagnetically conjugate-station records to obtain a comparative scenario of the Pc5 pulsation under SAMA influences. Thus, we analyzed the horizontal geomagnetic field components, H, measured on the ground and adequately filtered to obtain the Pc5 pulsations. We examined the pulsations applying mainly wavelet transform techniques to calculate pulsation spectral and coherence characteristics. The case study referred to a moderate geomagnetic storm on October 25 th to 26 th, 2016, a period close fortunately to an interhemispherical illumination symmetry, which partially mitigates the complexities from the morphology involving the plasmasphere-ionosphere region.

From a comprehensive approach using conjugate stations, we reach the main conclusions:

- The external cause of triggering Pc5-pulsation at middle-to-low latitude was the magnetopause compression by the solar wind pressure enhancements.
- The high-magnitude pulsation maintenance is associated with the magnetic field decreasing during a geomagnetic storm.
- In both globe regions, the dominant frequencies calculated (1.9, 2.1, 2.6, and 2.8 mHz) are consistent with values observed in earlier low-latitude studies.
- The Pc5 pulsations occur simultaneously and similarly between the conjugate stations in the Asia-Pacific region, while under the SAMA influence, there are dissimilarities.
- The Pc5-pulsation amplitudes present a systematic decrease with decreasing latitude or L-shell in the Asia-Pacific region. In contrast, in the Americ-SAMA region, the Northern station pulsations present behaviour similar to the Asia-Pacific stations and in the SAMA region, those pulsation patterns are not followed. Notably, for stations close to minima in the SAMA, higher amplitudes occur during the main phase of the geomagnetic storm or in significant magnetic decreases during recovery. Enhancements of Pc5-pulsation amplitudes occur associated with the probable electron precipitation into the higher ionosphere in the SAMA.
- In all conjugate stations in the Asia-Pacific region, the Pc5 pulsations were similar in amplitude, wave structure, and duration. The signals between conjugate pairs present high coherence and in-phase behavior. In the America-SAMA region, the Pc5 pulsations showed moderate to low signal coherences and phase lags.

As a general statement, although the Pc5 wave structures result similarly from the same external source, the plasmasphere-ionosphere system conditions in the America-SAMA region are less symmetrical than one in the Asia-Pacific region. For potential space weather purposes, it is verified that the morphological spatial characteristics affect the Pc5 pulsations in the magnetic line that interlinks conjugate stations. Besides, in the SAMA region, the electrodynamics of particle precipitations due to magnetic decrease in a magnetic storm are added to the electrical conductivity alterations of the ionosphere and the presence of electric fields.

This work characterizes and confirms essential differences between the Pc5-pulsation behavior affected by South Atlantic Magnetic Anomaly compared to an expected typical region outside, here an Asia-Pacific region. At last, an interesting suggestion is for researchers dealing with ionosphere data to investigate the role of internal causes, such as Field Line Resonance and cavity/waveguide modes, in modifying magnetic pulsations (a subject out of the scope of this work).

Appendix

Space Environment Conditions

Built from interplanetary data, Fig. 9 presents the space environment conditions and, from the ground measurements, the consequent geomagnetic effects on the ground. The plot's color region interval (between the vertical lines) corresponds to the Pc5 pulsation period under study. Obtained from the OMNI Web Service, NASA (https://omniweb.gsfc.nasa.gov/form/omni_min.html), the dataset in the panels of the left side consists of the northward-oriented interplanetary magnetic component B_z (in Geocentric Solar magnetospheric coordination system), the solar plasma speed V_x (from Sun to Earth), the numerical density of the solar particles N, the dynamic pressure P of the solar plasma incident upon the magnetosphere, which is the Earth's space region ruled by the geomagnetic field. The right-hand side panels show the geomagnetic disturbances in the higher latitudes, quantified by the Auroral Electroject geomagnetic index (related to the auroral ionospheric electric currents), and at lower latitudes, quantified by the Dst geomagnetic index, related to the ring current. They also show the Kp planetary geomagnetic index and Pc5 magnetic pulsations of KAK. More details about solar-terrestrial phenomenologies can be consulted in [14].

Establishing a physical interpretation of this plot, one can observe that at 06 : 00 UT, October 23th 2016, there is a starting of the negative-value Bz, which preserves this predominant orientation along the remaining time. This southward Bz determines an electrodynamic coupling between the solar wind and the Earth's magnetosphere, in a process of merging magnetic field lines known as magnetic reconnection. During this process, magnetic disturbances occur on Earth, as auroral activity seen in AE with values higher than 2000 nT, a geomagnetic storm in the index Dst decreasing until −52 nT, and a planetary disturbance index Kp increasing till 7. The last graph shows the Pc5 magnetic pulsations

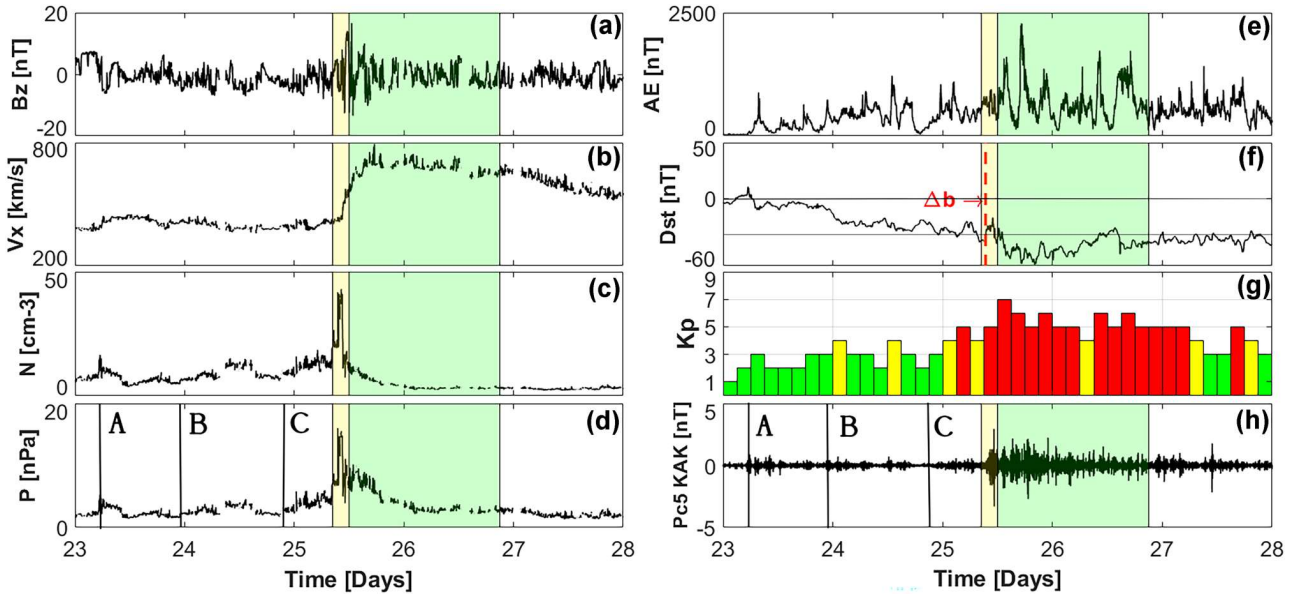

Fig. 9 Between Oct. 23 and 26, 2016, the space environment conditions and geomagnetic disturbance effects involving the Pc5-pulsation period (interval indicated by the vertical lines). **a** Interplanetary magnetic component B_z. **b** Solar plasma speed. **c** Numerical density of the solar particles. **d** Dynamic pressure. **e** Auroral Electroject geomagnetic index. **f** Dst geomagnetic index. **g** Kp geomagnetic index. **h** Pc5 magnetic pulsations of KAK. The dashed vertical line in plot Dst indicates the abrupt magnetic increase (Δb)

of KAK with a significant start after 09 : 00 UT, on October 25 th. Corresponding to the yellow color interval (between the two first vertical lines in the plots), a peculiar phenomenon occurs about at 09 : 00 UT, characterized by an abrupt increase of the solar plasma pressure, which compresses the magnetosphere and produces an abrupt magnetic increase (Δb) of the horizontal geomagnetic field at low latitudes, which occurred precisely at 09 : 22 UT on October 25 th. Vertical lines indicated by letters A, B, and C indicate compression examples (panel d) and the respective Pc5 pulsations triggered (panel h).

Acknowledgements This study was financed by the Coordenação de Aperfeiçoamento de Pessoal de Nível Superior (CAPES), grant $88882.447070/2019-01$ and PCI/INPE/MCTI grant $317943/2021-9$. O. Mendes thanks CNPq through grants $424352/2018-4$ and $307083/2017-9$. M.O. Domingues thanks CNPq through grant $306985/2021-7$ and Fapesp $2020/13015-0$. The authors would like to thank the INTERMAGNET (https://www.intermagnet.org), EMBRACE MagNet (http://www2.inpe.br/climaespacial/portal/en/), OMNI (https://cdaweb.gsfc.nasa.gov/) and WDC Kyoto programs (https://wdc.kugi.kyoto-u.ac.jp/wdc/Sec3.html) for the dataset used in this work.

Author Contributions All authors cooperate in the same proportion in the work.

Funding EC received from the Coordenação de Aperfeiçoamento de Pessoal de Nível Superior (CAPES), grant $88882.447070/2019-01$ and PCI/INPE/MCTI grant $317943/2021-9$, OM received from CNPq/MCTI through grants $424352/2018-4$ and $307083/2017-9$, and MO from CNPq/MCTI through grant $306985/2021-7$ and Fapesp $2020/13015-0$.

Data Availability Data are available from the international repositories (World Data Center-C, Tokyo; and OMNI Web Service, NASA) and from INPE Embrace's site.

Code Availability Codes are available from free(dom) software or with the methodology described.

Declarations

Ethics Approval The work followed better human and scientific practices.

Consent to Participate All participants consent to the work.

Consent for Publication All participants consent for publication.

Conflict of Interest The authors declare no competing interests.

References

1. K.A. Nasuddin, M. Abdullah, N.S. Abdul Hamid, Characterization of the South Atlantic Anomaly. Nonlinear Processes Geophys. **26**, 25–35 (2019). https://doi.org/10.5194/npg-26-25-2019
2. F.J. Pavón-Carrasco, A. De Santis, The South Atlantic Anomaly: The Key for a Possible Geomagnetic Reversal. Front. Earth Sci. **4**(40), 1–9 (2016). https://doi.org/10.3389/feart.2016.00040
3. R. Caraballo, The south atlantic magnetic anomaly phenomena: Its impact on the technological infrastructure. Master's thesis, University of the Republic Uruguay. (2016). https://doi.org/10.13140/RG.2.1.4345.5600
4. J. Domingos, D. Jault, M.A. Pais, M. Mandea, The South Atlantic Anomaly throughout the solar cycle. Earth Planet. Sci. Lett. **473**, 154–163 (2017). https://doi.org/10.1016/j.epsl.2017.06.004
5. S. Sanchez, J. Wicht, J. Baerenzung, Predictions of the geomagnetic secular variation based on the ensemble sequential assimilation of geomagnetic field models by dynamo simulations. Earth, Planets and Space **72**(157), 1–20 (2020). https://doi.org/10.1186/s40623-020-01279-y
6. G.A. Hartmann, I.G. Pacca, Time evolution of the South Atlantic Magnetic Anomaly. Anais da Academia Brasileira de Ciências **81**(2), 243–255 (2009). https://doi.org/10.1590/S0001-37652009000200010
7. O. Pinto Jr, W. Gonzalez, I. Pinto, A. Clua de Gonzalez, O. Mendes, The south atlantic magnetic anomaly: three decades of research. J. Atmos. Terr. Phys. **54**(9), 1129–1134 (1992). https://doi.org/10.1016/0021-9169(92)90137-A
8. F. Nichitiu, J.R. Drummond, J. Zou, R. Deschambault, Solar particle events seen by the MOPITT instrument. J. Atmos. Solar Terr. Phys. **66**(18), 1797–1803 (2004). https://doi.org/10.1016/j.jastp.2004.06.002
9. A. De Santis, E. Qamili, G. Spada, P. Gasperini, Geomagnetic South Atlantic Anomaly and global sea level rise: A direct connection? J. Atmos. Solar Terr. Phys. **74**, 129–135 (2012). https://doi.org/10.1016/j.jastp.2011.10.015
10. F. Terra-Nova, H. Amit, G. Hartmann, R. Trindade, K. Pinheiro, Relating the south atlantic anomaly and geomagnetic flux patches. Phys. Earth Planet. Inter. **266**, 39–53 (2017). https://doi.org/10.1016/j.pepi.2017.03.002
11. A. De Santis, E. Qamili, L. Wu, Toward a possible next geomagnetic transition? Nat. Hazard. **13**, 3395–3403 (2013). https://doi.org/10.5194/nhess-13-3395-2013
12. S.A. Campuzano, M. Gómez-Paccard, F.J. Pavón-Carrasco, M.L. Osete, Emergence and evolution of the South Atlantic Anomaly revealed by the new paleomagnetic reconstruction SHAWQ2k. Earth Planet. Sci. Lett. **512**, 17–26 (2019). https://doi.org/10.1016/j.epsl.2019.01.05
13. S.A. Campuzano, A. De Santis, F.J. Pavón-Carrasco, M.L. Osete, E. Qamili, New perspectives in the study of the earth's magnetic field and climate connection: The use of transfer entropy. PLOS ONE **13**(11), 0207270 (2018). https://doi.org/10.1371/journal.pone.0207270
14. M. Kivelson, C. Russell (eds.), *Introduction to Space Physics* (Cambridge University, Cambridge, 1995)
15. J. Matzka, N. Olsen, C.F. Maule, L.W. Pedersen, A. Berarducci, S. Macmillan, Geomagnetic observations on Tristan da Cunha. South Atlantic ocean. Annal of Geophysics **52**(1), 97–105 (2009). https://doi.org/10.4401/ag-4633
16. H.Y. Ye, Q. Zou Zong, H. Chen, Y. Wang, X. Yu, W. Shi, The Secular Variation of the Center of Geomagnetic South Atlantic Anomaly and Its Effect on the Distribution of Inner Radiation Belt Particles. Space Weather **15**(11), 1548–1558 (2017). https://doi.org/10.1002/2017SW001687
17. R. Caraballo, L.S. Bettucci, G. Tancredi, Geomagnetically induced currents in the uruguayan high-voltage power grid. Geophys. J. Int. **195**(2), 844–853 (2013). https://doi.org/10.1093/gji/ggt293
18. F. Terra-Nova, H. Amit, G. Choblet, Preferred locations of weak surface field in numerical dynamos with heterogeneous core-mantle boundary heat flux: Consequences for the South Atlantic Anomaly. Geophys. J. Int. **217**(2), 1179–1199 (2019). https://doi.org/10.1093/gji/ggy519
19. C. Finlay, C. Kloss, N. Olsen, M. Hammer, L. Tøffner-Clausen, A. Grayver, A. Kuvshinov, The CHAOS-7 geomagnetic field model and observed changes in the South Atlantic Anomaly. Earth, Planets and Space **72**(156), 1–31 (2020). https://doi.org/10.1186/s40623-020-01252-9

20. A. Du, G. Chen, W. Xu, M. Hong, H. Chen, F. Peng, Characteristics of the Pc5 ULF waves during the magnetic storm on July 15–16, 2000. Chin. J. Geophys. **46**(3), 457–464 (2003). https://doi.org/10.1002/cjg2.3363
21. Y. Kamide, A. Chian (eds.), *Handbook of the Solar-terrestrial Environment* (Springer-Verlag, Berlin, 2007)
22. X. Shi, J. Ruohoniemi, J. Baker, D. Lin, E. Bland, M. Hartinger, W. Scales, Survey of ionospheric Pc3-5 ULF wave signatures in super-DARN high time resolution data. J. Geophys. Res. Space Physics **123**(5), 4215–4231 (2018). https://doi.org/10.1029/2017JA025033
23. C.T. Russell, J.G. Luhmann, R.J. Strangeway, *Space Physics an Introduction*, 1st edn. (Cambridge University, Cambridge, 2016)
24. K. Takahashi, ULF waves in the inner magnetosphere. Low-frequency waves in space plasmas, 1st. edn. Geophysical Monograph **216**, 53–63 (2016). AGU & John Wiley, New Jersey
25. J. Kangas, A. Guglielmi, O. Pokhotelov, Morphology and physics of short-period magnetic pulsations. Space Sci. Rev. **83**(3–4), 435–512 (1998). https://doi.org/10.1023/A:1005063911643
26. D. Orr, Magnetic pulsations within the magnetosphere: A review. J. Atmos. Terr. Phys. **35**(1), 1–50 (1973). https://doi.org/10.1016/0021-9169(73)90214-6
27. V. Troitskaya, A. Gul'Elmi, Geomagnetic micropulsations and diagnostics of the magnetosphere. Space Sci. Rev. **7**, 689–768 (1967). https://doi.org/10.1007/BF00542894
28. L.G. Blomberg, Mercury's magnetosphere, exosphere and surface: low-frequency field and wave measurements as a diagnostic tool. Planet. Space Sci. **4**(1), 143–148 (1997). https://doi.org/10.1016/S0032-0633(96)00092-X
29. V. Pilipenko, O. Kozyreva, V. Belakhovsky, M.J. Engebretson, S. Samsonov, Generation of magnetic and particle Pc5 pulsations during the recovery phase of strong magnetic storms. Proceedings of the Royal Society A **466**, 3363–3390 (2010). https://doi.org/10.1098/rspa.2010.0079
30. Y. Obana, A. Yoshikawa, J.V. Olson, R.J. Morris, B. Fraser, K. Yumoto, North-south asymmetry of the amplitude of high-latitude Pc3-5 pulsations: Observations at conjugate stations. J. Geophys. Res. Space Phys. **110**(A10), 10214–19 (2005). https://doi.org/10.1029/2003JA010242
31. M. Hudson, R. Denton, M. Lessard, E. Miftakhova, R. Anderson, A study of Pc-5 ULF oscillations. Ann. Geophys. **22**(1), 289–302 (2004). https://doi.org/10.5194/angeo-22-289-2004
32. K. Takahashi, B. Anderson, P. Newell, T. Yamamoto, N. Sato, Propagation of compressional Pc3 pulsations from space to the ground: A case study using multipoint measurements. Solar Wind Sources of Magnetospheric Ultra-Low-Frequency Waves. Geophysical Monograph. **81**, 355–363 (1994). American Geophysical Union, Washington DC. https://doi.org/10.1029/GM081p0355
33. R. McPherron, Magnetic pulsations: their sources and relation to solar wind and geomagnetic activity. Surv. Geophys. **26**, 545–592 (2005). https://doi.org/10.1007/s10712-005-1758-7
34. V.B. Belakhovsky, V.A. Pilipenko, Generation of magnetic field pc5 pulsations and particle fluxes during the recovery phase of a magnetic storm on october 31, 2003. Geomagn. Aeron. **51**(599) (2011). https://doi.org/10.1134/S0016793211040050
35. L. Cahill, J. Winckler, Periodic magnetopause oscillations observed with the GOES satellites on march 24, 1991. J. Geophys. Res. Space Physics **97**(A6), 8239–8243 (1992). https://doi.org/10.1029/92JA00433
36. D. Oliva, M. Meirelles, A. Papa, A study of Pc4-5 geomagnetic pulsations in the Brazilian sector. Physics Space, 1–17 (2014). 10.48550/arXiv.1404.4321
37. T. Saito, K. Yumoto, Y. Koyama, Magnetic pulsation pi2 as a sensitive indicator of magnetospheric substorm. Planet. Space Sci. **24**(11), 1025–1029 (1976). https://doi.org/10.1016/0032-0633(76)90120-3
38. O.V. Agapitov, O.K. Cheremnykh, Magnetospheric ULF waves driven by external sources. Adv. Astron. Space Phys. **3**, 12–19 (2013). www.aasp.kiev.ua/volume3/012-019-Agapitov.pdf
39. Y. Liu, B. Fraser, R. Liu, P. Ponomarenko, Conjugate phase studies of ULF waves in the Pc5 band near the cusp. J. Geophys. Res. Space Phys. **108**(A7) (2003). https://doi.org/10.1029/2002JA009336
40. W. Allan, E.M. Poulter, ULF waves-their relationship to the structure of the Earth's magnetosphere. Rep. Prog. Phys. **55**(5), 533 (1992). https://doi.org/10.1088/0034-4885/55/5/001
41. C. Waters, B. Harrold, F. Menk, J. Samson, B. Fraser, Field line resonances and waveguide modes at low latitudes: 2. a model. J. Geophys. Res. Space Phys. **105**(A4), 7763–7774 (2000). https://doi.org/10.1029/1999JA900267
42. A. Du, W. Sun, W. Xu, The frequency variation of Pc5 ULF waves during a magnetic storm. Earth, Planets and Space **57**, 619–625 (2005). https://doi.org/10.1186/BF03351841
43. H. Saito, N. Sato, Y. Tonegawa, T. Yoshino, T. Saemundsson, Seasonal and diurnal dependence of Pc 3–5 magnetic pulsation power at geomagnetically conjugate stations in the auroral zones. J. Geophys. Res. Space Physics **94**(A6), 6945–6948 (1989). https://doi.org/10.1029/JA094iA06p06945
44. S. Takasaki, N. Sato, A. Kadokura, H. Yamagishi, H. Kawano, Y. Ebihara, Y. Tanaka, Interhemispheric observations of field line resonance frequencies as a continuous function of ground latitude in the auroral zones. Polar Sci. **2**(2), 73–86 (2008). https://doi.org/10.1016/j.polar.2008.05.003
45. E. Wescott, Magnetoconjugate phenomena. Space Sci. Rev. **5**, 507–561 (1966). https://doi.org/10.1007/BF00240576
46. T. Nagata, Geomagnetic conjugacy between the antarctic and the arctic. In: Proceedings of the International Symposium on Pacific Antarctic Sciences Pacific, Pacific Science Congress, 11th., pp. 65–80. National Institute of Polar Research Repository, Tokyo (1967). https://core.ac.uk/download/51479527.pdf
47. T. Nagata, S. Kokubun, N. Fukushima, Similarity and simultaneity of magnetic disturbance in the northern and southern hemispheres. J. Phys. Soc. Jpn. 17(Supplement A-I), 17–35 (1962). http://adsabs.harvard.edu/abs/1962JPSJS..17A..35N
48. E. Wescott, Magnetic variations at conjugate points. J. Geophys. Res. **66**(6), 1789–1792 (1961). https://doi.org/10.1029/JZ066i006p01789
49. Z. Mtumela, J.A. Stephenson, A.D. Walker, An investigation of the nature of a Pc5 pulsation event using SuperDARN and magnetometer data. S. Afr. J. Sci. **111**(3/4), 1–7 (2015). https://doi.org/10.17159/sajs.2015/20130391
50. E. Wescott, K. Mather, Magnetic conjugacy at very high latitude; shepherd bay-scott base relationship. Planet. Space Sci. **13**(4), 303–324 (1965). https://doi.org/10.1016/0032-0633(65)90005-X
51. E. Wescott, K. Mather, Magnetic conjugacy from $l = 6$ to $l = 1.4$: 1. auroral zone: Conjugate area, seasonal variations, and magnetic coherence. J. Geophys. Res. **70**(1), 29–42 (1965). https://doi.org/10.1029/JZ070i001p00029
52. L. Hajkowicz, Magnetoconjugate phenomena in alaska and macquarie is., australia in 2003: position of the global maximum isoaurorae. Ann. Geophys. **24**, 2611–2617 (2006). https://doi.org/10.5194/angeo-24-2611-2006
53. K. Yumoto, T. Saito, Y. Tanaka, Low-latitude Pc3 magnetic pulsations observed at conjugate stations ($l \sim 1.5$. J. Geophys. Res. Space Phys. **90**(A12), 12201–12207 (1985). https://doi.org/10.1029/JA090iA12p12201
54. J. Schott, N. Kleimenova, O. Bitterly, The strong pc5 geomagnetic pulsations in the initial phase of the great magnetic storm of march 24, 1991. Earth, Planets and Space **50**, 101–106 (1998). https://doi.org/10.1186/BF03352091
55. M.D. Hartinger, Z. Xu, C.R. Clauer, Y. Yu, D.R. Weimer, H. Kim, V. Pilipenko, D.T. Welling, R. Behlke, A.N. Willer, Associating ground magnetometer observations with current or voltage generators. J. Geophys. Res. Space Physics **122**(7), 7130–7141 (2017). https://doi.org/10.1002/2017JA024140
56. E. Timoçin, I. Ünal, Y. Tulunay, U.D. Göker, The effect of geomagnetic activity changes on the ionospheric critical frequencies

(fof2) at magnetic conjugate points. Adv. Space Res. **62**(4), 821–828 (2018). https://doi.org/10.1016/j.asr.2018.05.035
57. S. Shepherd, Altitude-adjusted corrected geomagnetic coordinates: Definition and functional approximations. J. Geophys. Res. Space Physics **119**(9), 7501–752 (2014). https://doi.org/10.1002/2014JA020264
58. K. Laundal, A.D. Richmond, Magnetic coordinate systems. Space Sci. Rev. **206**(1–4), 27–59 (2017). https://doi.org/10.1007/s11214-016-0275-y
59. C.M. Denardini, S.S. Chen, L.C.A. Resende, J. Moro, A.V. Bilibio, P.R. Fagundes, M.A. Gende, M.A. Cabrera, M.J.A. Bolzan, A.L. Padilha, N.J. Schuch, J.L. Hormaechea, L.R. Alves, P.F. Barbosa Neto, P.A.B. Nogueira, G.A.S. Picanço, T.O. Bertollotto, The Embrace magnetometer network for South America: Network description and its qualification. Radio Sci. **53**(3), 288–302 (2018). https://doi.org/10.1002/2017RS006477
60. G. Balasis, I.A. Daglis, I.R. Mann (eds.), Waves, Particles, and Storms in Geospace: A Complex Interplay. Oxford Academic, Oxford (2016). https://doi.org/10.1093/acprof:oso/9780198705246.001.000
61. A. Zanandrea, J. Da Costa, S. Dutra, N. Trivedi, T. Kitamura, K. Yumoto, O. Saotome, Pc3-4 geomagnetic pulsations at very low latitude in Brazil. Planet. Space Sci. **52**(13), 1209–1215 (2004). https://doi.org/10.1016/j.pss.2004.08.001
62. O. Brigham, *The Fast Fourier Transform and Its Applications* (Prentice Hall, New Jersey, 1988)
63. I. Daubechies, Ten Lectures on Wavelets. Society for Industrial and Applied Mathematics, Philadelphia (1992). https://doi.org/10.1137/1.9781611970104
64. J. Antoine, R. Murenzi, P. Vandergheynst, S. Ali, (eds.), Two-Dimensional Wavelets and Their Relatives. Cambridge University, Cambridge (2004). https://doi.org/10.1017/CBO9780511543395
65. J. Olson, C. Szuberla, A study of Pc 3 coherence at cusp latitudes. J. Geophys. Res. Space Physics **102**(A6), 11375–11383 (1997). https://doi.org/10.1029/97JA00750
66. R. Bortel, P. Sovka, Approximation of statistical distribution of magnitude squared coherence estimated with segment overlapping. Signal Process. **87**(5), 1100–1117 (2007). https://doi.org/10.1016/j.sigpro.2006.10.003
67. D.S. Bloomfield, R.T.J. McAteer, B.W. Lites, P.G. Judge, M. Mathioudakis, F.P. Keenan, Wavelet phase coherence analysis: Application to a quiet-sun magnetic element. Astrophys. J. **617**, 623–632 (2004) https://iopscience.iop.org/article/10.1086/425300/pdf
68. A. Grinsted, J. Moore, S. Jevrejeva, Application of the cross wavelet transform and wavelet coherence to geophysical time series. Nonlinear Process. Geophys. **11**, 561–566 (2004). https://doi.org/10.5194/npg-11-561-2004
69. C. Torrence, G.P. Compo, A practical guide to wavelet analysis. Bull. Am. Meteorol. Soc. **79**(1), 61–78 (1998). https://doi.org/10.1175/1520-0477(1998)079<0061:APGTWA>2.0.CO;2
70. D. Labat, Recent advances in wavelet analyses: Part 1. a review of concepts. J. Hydrol. **314**(1–4), 275–288 (2005). https://doi.org/10.1016/j.jhydrol.2005.04.003
71. C.W. Jun, K. Shiokawa, M. Connors, I. Schofield, I. Poddelsky, B. Shevtsov, Study of Pc1 pearl structures observed at multi-point ground stations in Russia, Japan, and Canada. Earth, Planets and Space **66**(1), 1–14 (2014). https://doi.org/10.1186/s40623-014-0140-8
72. C.W. Jun, K. Shiokawa, M. Connors, I. Schofield, I. Poddelsky, B. Shevtsov, Possible generation mechanisms for Pc1 pearl structures in the ionosphere based on 6 years of ground observations in Canada, Russia, and Japan. J. Geophys. Res. Space Physics **121**(5), 4409–4424 (2016). https://doi.org/10.1002/2015JA022123
73. T. Oguti, Conjugate point problems. Space Sci. Rev. **9**, 745–804 (1969). https://doi.org/10.1007/BF00226262
74. Y. Tonegawa, H. Fukunishi, Harmonic structure of Pc3-5 magnetic pulsations observed at the Syowa-Husafell conjugate pair. J. Geophys. Res. Space Physics **89**(A8), 6737–6748 (1984). https://doi.org/10.1029/JA089iA08p06737
75. B.M. Pathan, N.G. Kleimenova, O.V. Kozyreva, D.R.K. Rao, R.L. Asinkar, Equatorial enhancement of Pc5-6 magnetic storm time geomagnetic pulsations. Earth, Planets and Space **51**(9), 959–964 (1999). https://doi.org/10.1186/BF03351566
76. J.C. Gupta, Some features of pc5 pulsations in the period range 180–300 sec. J. Geomag. Geoelec. **28**(5), 359–373 (1976). https://doi.org/10.5636/jgg.28.359
77. F.W. Menk, B.J. Fraser, C.L. Waters, C.W.S. Ziesolleck, Q. Feng, S.H. Lee, P.W. Mcnabb, Ground Measurements of Low Latitude Magnetospheric Field Line Resonances. Solar Wind Sources of Magnetospheric Ultra-Low-Frequency Waves, vol. 81, pp. 299–310. American Geophysical Union, Washington DC (1994). https://doi.org/10.1029/GM081p0299
78. G. Da Silva, A. Padilha, L. Alves, Latitudinal variation of Pc3-Pc5 geomagnetic pulsation amplitude across the dip equator in central South America. Ann. Geophys. **38**, 35–49 (2020). https://doi.org/10.5194/angeo-38-35-2020
79. A. Boudouridis, E. Zesta, Comparison of fourier and wavelet techniques in the determination of geomagnetic field line resonances. J. Geophys. Res. Space Physics **112**(A8), 1–8 (2007). https://doi.org/10.1029/2006JA011922
80. V. Belakhovsky, V. Pilipenko, D. Murr, E. Fedorov, A. Kozlovsky, Modulation of the ionosphere by pc5 waves observed simultaneously by gps/tec and eiscat. Earth, Planets and Space **68**(1) (2016). https://doi.org/10.1186/s40623-016-0480-7
81. N. Trivedi, B. Abdu, M. Pathan, S. Dutra, N. Schuch, J. Santos, L. Barreto, Amplitude enhancement of SC (H) events in the South Atlantic anomaly region. J. Atmos. Sol. Terr. Phys. **67**(17–18), 1751–1760 (2005). https://doi.org/10.1016/j.jastp.2005.03.010
82. N. Trivedi, B. Pathan, N.J. Schuch, M. Barreto, L. Dutra, Geomagnetic phenomena in the South Atlantic anomaly region in Brazil. Adv. Space Res. **36**(10), 2021–2024 (2005). https://doi.org/10.1016/j.asr.2004.09.020
83. C.W.S. Ziesolleck, F.H. Chamalaun, A two-dimensional array study of low latitude pc5 geomagnetic pulsations. J. Geophys. Res. Space Physics **98**(A8), 13703–13713 (1993). https://doi.org/10.1029/93JA00637
84. P. Francia, U. Villante, Some evidence of ground power enhancements at frequencies of global magnetospheric modes at low latitude. Ann. Geophys. **15**(1), 17–23 (1997). https://doi.org/10.1007/s00585-997-0017-2
85. U. Villante, P. Francia, S. Lepidi, Pc5 geomagnetic field fluctuations at discrete frequencies at a low latitude station. Ann. Geophys. **19**(3), 321–325 (2001). https://doi.org/10.5194/angeo-19-321-2001
86. P. Francia, S. Lepidi, U. Villante, Low latitude geomagnetic field fluctuations at discrete frequencies as possible indicators for global magnetospheric oscillations. Memorie della Societa Astronomica Italiana **72**, 606–613 (2001). https://www.researchgate.net/publication/234500334_Low_latitude_geomagnetic_field_fluctuations_at_discrete_frequencies_as_possible_indicators_for_global_magnetospheric_oscillations
87. M. Abdu, I. Batista, A. Carrasco, C. Brum, South Atlantic magnetic anomaly ionization: A review and a new focus on electrodynamic effects in the equatorial ionosphere. J. Atmos. Solar Terr. Phys. **67**, 1643–1657 (2022). https://doi.org/10.1016/j.jastp.2005.01.014
88. N. Balan, L. Liu, H. Le, A brief review of equatorial ionization anomaly and ionospheric irregularities. Earth and Planetary Physics **2**(4), 1–19 (2018). https://doi.org/10.26464/epp2018025
89. X. Luan, Equatotial ionization anomaly variations during geomagnetic storms. Ionosphere dynamics and applications. Geophysical Monograph, pp. 301–312. American Geophysical Union, Washington DC (2021). https://doi.org/10.1002/9781119815617.ch13